ACS APPLIED MATERIALS & INTERFACES

Letter

www.acsami.org

Electroless Copper Plating of Inkjet-Printed Polydopamine Nanoparticles: a Facile Method to Fabricate Highly Conductive Patterns at Near Room Temperature

Siyuan Ma,[†] Liang Liu,[†] Vadim Bromberg,[‡] and Timothy J. Singler*,[†]

[†]Department of Mechanical Engineering, State University of New York (SUNY) at Binghamton, Binghamton, New York 13902, United States

[‡]Additive Manufacturing Lab, GE Global Research, Niskayuna, New York 12309, United States

Supporting Information

ABSTRACT: Aqueous dispersions of artificially synthesized, mussel-inspired poly(dopamine) nanoparticles were inkjet printed on flexible polyethylene terephthalate (PET) substrates. Narrow line patterns (4 μm in width) of poly(dopamine) resulted due to evaporatively driven transport (coffee ring effect). The printed patterns were metallized via a site-selective Cu electroless plating process at a controlled temperature (30 °C) for varied bath times. The lowest electrical resistivity value of the plated Cu lines was about 6 times greater than the bulk resistivity of Cu. This process presents an industrially viable way to fabricate Cu conductive fine patterns for flexible electronics at low temperature, low cost, and without need of sophisticated equipment.

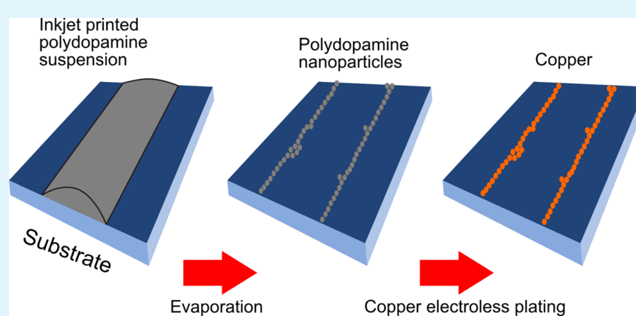

KEYWORDS: *inkjet printing, mussel-inspired material, polydopamine site-selective electroless plating, low temperature metallization, coffee-ring, twin line*

Emerging flexible electronic devices have exhibited significant potential for a wide range of applications such as solar cells,[1] batteries,[2] sensors,[3] antennas,[4] and displays.[5] For any flexible electronic application, an essential characteristic is electrically conductive patterning. Solution-based additive manufacturing techniques such as drop-on-demand (DOD) inkjet printing,[6] slot die coating,[7] and gravure printing[8] are being widely investigated to fabricate flexible conductive patterns. DOD inkjet printing is an excellent candidate because it is a material-conservative, low-temperature process and is easily incorporated into large scale roll-to-roll (R2R) manufacturing infrastructures for flexible polymer substrates.

The commonly used ink materials in DOD inkjet printing processes can be categorized into two types: metal nanoparticle (NP) dispersions and metal precursor solutions.[9] NP inks consist of metallic NPs and a carrier liquid solvent. The NPs have specifically designed surface properties which allow them to be stably dispersed in an appropriate solvent. Precursor ink is an inorganic metal salt or organic metal complex that is dissolved in a solvent. After inkjet printing, the solvent undergoes evaporation and metal NP or precursor deposits on the substrate. A postprinting process is typically necessary to render either type of deposited structure electrically conductive. Polymer capping layers and surfactants are employed in the formulation of NP inks to prevent aggregation and particle precipitation; these agents are generally neither conductive nor volatile. The postprinting process removes these agents and initiates sintering, thereby improving the electrical conductivity. For precursor inks, the postprinting process chemically reduces the metal species from its ionic to elemental state which is electrically conductive. The standard postprinting process applies heat that potentially puts substrate materials at risk of thermal degradation/deformation, especially when low-cost polymeric substrates are used (e.g., polyethylene terephthalate (PET), etc.). A few nonthermal or local surface thermal techniques have been reported including plasma,[10,11] laser,[12] electrical,[13] and photonic[14] methods. However, sophisticated equipment and their associated high-cost processes are inevitable.

Silver (Ag) is the most broadly investigated conductive ink material due to its low bulk resistivity (1.6×10^{-8} Ω m) and resistance to oxidation; however, like other noble metals, it is expensive ($0.708/gram).[15] Copper (Cu) is preferred because it exhibits a bulk resistivity (1.7×10^{-8} Ω m) comparable to Ag but is significantly cheaper ($0.007/gram).[15] However, the main challenge of using Cu-based raw material for inkjet printing arises from the spontaneous formation of Cu oxides; when synthesized Cu NPs oxidize, both their resistivity and sintering temperature increase dramatically.[9] Research efforts to overcome the Cu NP oxidation have taken two directions:

Received: September 9, 2014
Accepted: October 31, 2014
Published: October 31, 2014

ACS Publications © 2014 American Chemical Society

utilizing an organic oxygen barrier material as particle capping layers to retard oxidation kinetics[16] and synthesis of Cu−noble metal core−shell NPs to achieve long-term stability.[17] Cu precursor inks are usually stable against oxidation under room environment.[18] Notwithstanding, the postprinting process for both Cu NP and Cu precursor must be implemented in reductive, inert atmospheres or under vacuum to prevent oxide formation, which inherently increases process complexity.[19]

Site-selective Cu electroless plating (ELP) is a method that can be used to fabricate conductive patterns on flexible substrates. It is a low temperature process that does not cause substrate damage if a proper plating bath is used. During ELP, formation of Cu oxides is dramatically inhibited. The general ELP uses a solution of metal salt, complexing agent, reducing agent and additive(s) (such as a bath stabilizer and a pH adjusting agent).[20] Metal nucleates on a catalytically active surface on which further metal reduction and growth occurs. This is the intrinsic autocatalytic nature of the ELP process. Site-selective ELP can be achieved by plating a substrate which has a prepatterned catalyst/seed layer. Studies have been conducted exploring inkjet printing for ELP seed patterning.[21−23] The Pd-based ink is the most widely investigated material due to its well-established catalytic activity for initiation of various metal deposition from a wide range of ELP solutions.[24] However, the suitability of Pd-based inks is limited by their substrate-dependent adhesion.[21−23] Additionally, the high price of Pd prohibits its use in many applications.[25]

Poly(dopamine) (PDA), a marine mussel inspired polymer, was recently found capable of initiating metal ion reduction indicating its potential as an ELP catalyst.[26] PDA exhibits universal adhesion as demonstrated for a wide range of both organic and inorganic materials.[26] PDA can be synthesized as continuous coatings on any object by inducing dopamine polymerization in a pure water phase[26] or as suspended spherical NPs in water−alcohol mixtures at controlled pH.[27]

In our previous work, we inkjet printed poly(dopamine) nanoparticles (PDA-NP) on both glass and PET substrates followed by site-selective Ag ELP.[28] Results exhibit a substrate-independent method to fabricate highly conductive Ag patterns. However, possibilities of extending this approach to other conductive metal systems (such as Cu) have not been investigated.

In this study, we report the effect of site-selective Cu plating conditions on the morphology and electrical resistivity of inkjet printed PDA-NP lines on polyethylene terephthalate (PET) substrates. The influences of cyclic bending on adhesion and air exposure on Cu lines are assessed.

PDA-NP was synthesized according to a published protocol[27] with minor modification (see the Supporting Information). The ink was formulated by mixing PDA-NP with distilled deionized (DI) water at a concentration of 0.25 wt % followed by 10 min ultrasonication (3510, Branson). The particle size distribution and zeta potential were characterized by dynamic light scattering (DLS) (ZetasizerNano, Malvern). The PDA-NP average diameter was about 340 ± 55 nm. The zeta potential of PDA-NP was measured as −31.0 ± 0.5 mV, indicative of good stability of the ink dispersion. Particle precipitation was not observed over a 30-day period.

The viscosity and surface tension were measured as 1.0 ± 0.1 mPa·s by a rotary viscometer (TA1000, TA Instruments) and 72.1 ± 0.1 mN m^{-1} by a bubble tensiometer (BP100, Kruss), respectively. These values were close to those of pure water due to the very small PDA-NP loading.

A single-nozzle inkjet printer was used to print the PDA-NP suspension onto plasma-treated PET substrates (Melinex ST506, Dupont) to form arrays of five lines (see the Supporting Information). After printing and solvent evaporation, PDA-NPs assembled into a pair of continuous lines with a minimal amount of noncontinuous deposition within the region between the line pair (Figure 1a). This phenomenon is caused

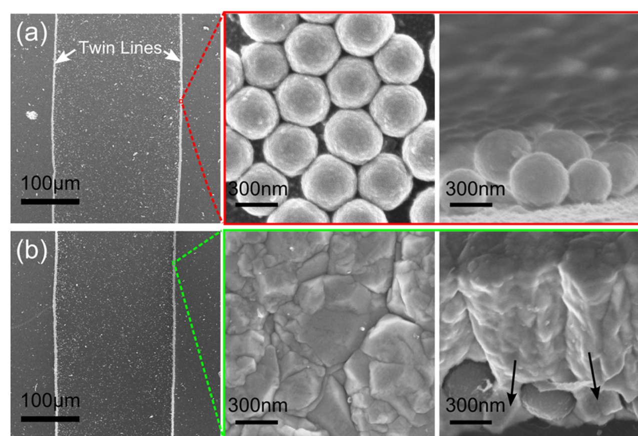

Figure 1. Typical scanning electron microscope (SEM) images of (a) printed lines of polydopamine nanoparticles and (b) lines subject to 15 min copper electroless plating, respectively. The lines indicate the approximate regions that are shown at higher magnification from both top and cross-sectional perspectives. The arrows in the cross-sectional SEM image of the copper plated lines indicate penetration of copper into the interstitial space of the polydopamine nanoparticle layer.

by a convective flow driven by nonuniform evaporation from the liquid/air interface, and was extensively studied for drops and referred to as the "coffee ring effect".[29] In our previous study, we defined this pair of lines as twin lines due to their similarity.[28,30] The width of a typical as-printed PDA-NP twin line was measured as 3.9 ± 0.6 μm in this study.

A potential mechanism of PDA-induced ELP has been suggested to involve the electrostatic interaction of metallic ions with surface catechol groups of PDA followed by catechol oxidation to quinone and reduction of metallic ions to elemental metal.[26] The newly deposited elemental metal further catalyzes the redox reaction for continuous deposition. In this study, Cu ELP was performed by immersing the printed PDA patterns in a chemical bath at 30 °C for different durations (see the Supporting Information).

The morphology of the printed twin line before and after the plating process was characterized by scanning electron microscopy (SEM) (Supra 55VP, Zeiss) from both top and cross-sectional perspectives. For the as-deposited lines, each twin line typically consists of a single-particle thick PDA-NP structure. After 15 min of Cu ELP, a layer of Cu was plated on top of the PDA-NPs with some penetration into the interstitial space of the PDA-NP layer (Figure 1b). The plated Cu layer exhibited continuous structure with large grain size. It is also worth noting that no line width broadening was observed after Cu ELP.

Cu thickness was measured by the analysis of the cross-sectional SEM images. The thickness value is exhibited in Figure 2a based on the average of at least 8 different cross-sectional SEM pictures at each ELP time. The metal thickness

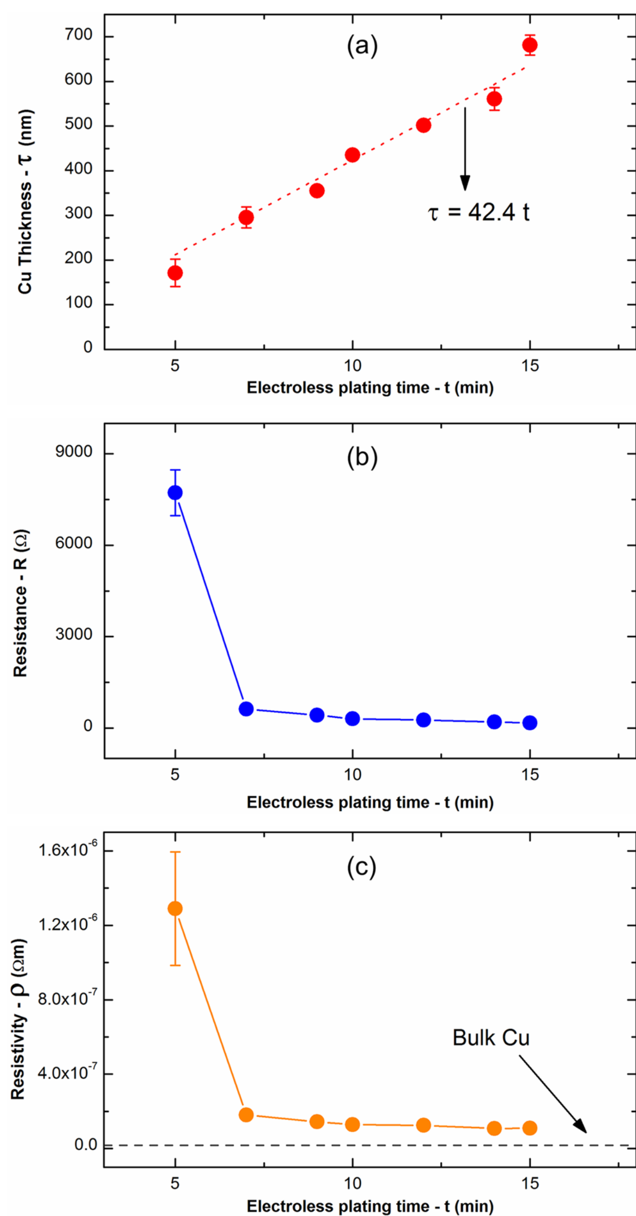

Figure 2. Structural and electrical performance characterization of deposit: (a) Cu thickness (τ) evolution; (b) individual twin line resistance; (c) individual twin line resistivity change as a function of Cu electroless plating time (t).

increased linearly with increasing ELP time. The plating rate of the Cu ELP process was measured to be about 42 nm/min. A maximum thickness of 682 ± 23 nm was achieved at the 15 min plating time.

The electrical resistance of each array of plated lines was assessed by a method we previously reported[28,30] (see the Supporting Information). The average resistance of each twin line after ELP processes is shown in Figure 2b. The minimum time required to achieve a conductive structure was approximately 5 min with a large resistance value of about 7722 Ω. The resistance decreased significantly to about 724 Ω for an ELP time of 10 min. The resistance then decreased slowly with increased plating time to a final resistance of 165 Ω for an ELP time of 15 min. The resistivity of each twin line was calculated according to $\rho = Rw\tau L^{-1}$ where ρ is the resistivity, R the line resistance, w the line width, τ the thickness, and L the length, respectively. The calculated resistivity values are shown in Figure 2c. The resistivity values decrease with increasing ELP time and the trend is similar to the resistance change shown in Figure 2b. The lowest resistivity value achieved after 15 min ELP was 1.1×10^{-7} Ω m, a value approximately 6 times that of bulk Cu.

Materials composition was confirmed by X-ray diffraction (XRD) (XDS2000, Scintag) as shown in Figure 3. The broad

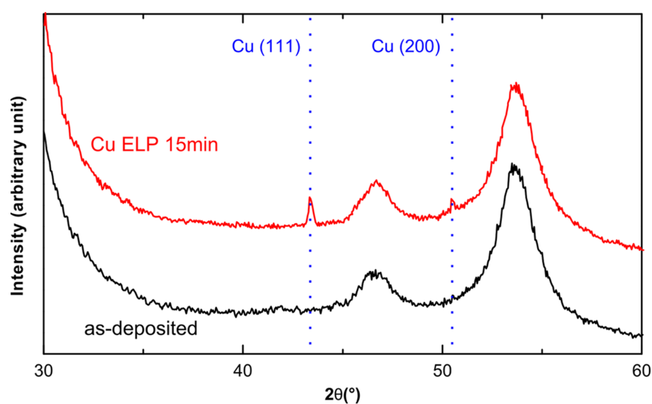

Figure 3. X-ray diffraction results of the printed polydopamine nanoparticle arrays before and after 15 min Cu electroless plating. The dotted lines indicate 2θ values of face-centered-cubic copper according to the Joint Committee on Powder Diffraction Standards (JCPDS) file 04–0836.

diffraction peaks occurring at 2θ angles of approximately 47 and 54° are attributable to the PET substrates.[31] The existence of printed PDA-NP lines does not introduce any additional diffraction patterns. For the patterns after 15 min Cu ELP, two characteristic diffraction peaks were exhibited associated with face-centered-cubic Cu crystalline at 43 and 51° (for Cu (111) and (200) planes, respectively). The 2θ locations of the diffraction peaks are consistent with the Joint Committee on Powder Diffraction Standards (JCPDS) file 04–0836. The XRD characterizations were all conducted within 30 min of the completion of the Cu ELP process. The absence of the diffraction peaks of cuprous or cupric oxide is perhaps due to the small amount of native oxide that is undetectable. Additional oxide characterization was beyond the primary focus of this study.

The bending robustness of Cu patterns was assessed using a cyclic bending test. During each cycle, the substrate was cyclically bent between concave and convex geometries with known radius of curvature (2.5 mm or 5 mm). The number of cycles ranged from 1000 to 10000, while the bending frequency was maintained at 100 cycles/min. The resistance of each line versus number of bending cycles is shown in Figure 4a. All the test samples were plated for 15 min. Only a slight increase of resistance with cycles was observed when the 5 mm bending radius was applied (Figure 4a). The resistance increases from the as-plated value 165 to 170 Ω (about 5% increase). For the 2.5 mm bending radius, the resistance value increased to 187 Ω, a 13% increase compared to the value prior to bending. The resistance increase due to bending is likely due to the formation of cracks as shown in Figure 4a (SEM images).

The adhesion of the plated metal lines was assessed qualitatively by a tape peel test. Briefly, a tape (Scotch600, 3M) was carefully adhered to the patterns and subsequently removed by peeling it off parallel to the substrate. Then the

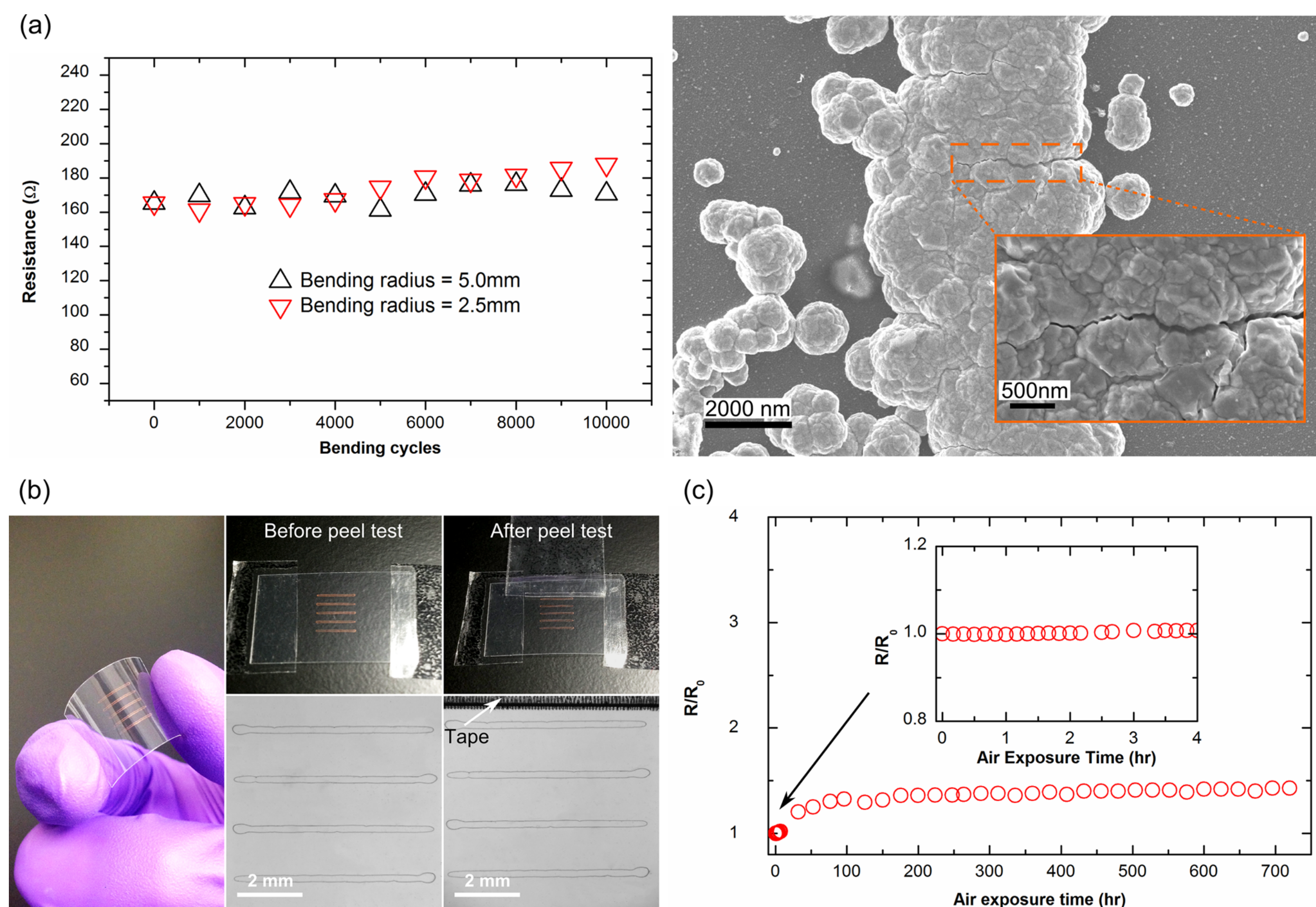

Figure 4. Robustness characterization of the inkjet printed polydopmaine nanoparticle (PDA-NP) lines followed by 15 min Cu electroless plating: (a) Twin line resistance change after cyclic bending (SEM images show the formation of cracks after 10000 bending cycles with 2.5 mm bending radius); (b) tape peel adhesion test; (c) influence of air exposure time on plated line resistance (R) relative to its as-plated resistance (R_0) (the inset is the first 4 h air exposure result as indicated by the arrow).

remaining patterns were observed by an optical microscope (AxioObserver A1, Zeiss). The plated lines (15 min Cu ELP) demonstrate good adhesion on PET substrates (Figure 4b). Subsequent to adhesive tape attachment and removal, no evidence of delamination or structural change was observed. Furthermore, there was no apparent degradation of adhesion after 10000 bending cycles.

Figure 4c shows the resistance as a function of air exposure time in a room environment. The Cu lines were formed by ELP for 15 min. Cu line resistance increases gradually to a value 1.43 times its as-plated value after 720 h. The likely reason is the formation of Cu oxides when elemental Cu is exposed to air. The resistance within the first 4 h of air exposure shows no increase relative to its as-plated resistance (Figure 4c, inset). It confirms that the Cu line resistance increase shown in the cyclic bending test (Figure 4a) was not influenced by air exposure as the bending test and the resulting resistance measurement were completed within 2.5 h. Inhibiting long-term air oxidation is necessary for practical applications and is still under investigation.

In conclusion, fine lines of Cu with low electrical resistivity were fabricated by sequential inkjet printing of an aqueous dispersion of mussel-inspired poly(dopamine) nanoparticles and site-selective electroless plating. The process forms Cu lines with thickness linearly dependent on plating time, and with an electrical resistivity 6 times that of bulk Cu. The resistance of the Cu lines does not change significantly with cyclic bending characterized by a 5 mm bending radius. The resistance of Cu lines increases over long-time storage, probably because of oxidation. This process demonstrates a simple, low temperature and low-cost method of fabricating fine conductive Cu patterns for flexible electronics applications.

■ ASSOCIATED CONTENT

Supporting Information

Details of materials, polydopamine nanoparticle (PDA-NP) synthesis, PDA-NP size characterization, substrate preparation, inkjet printing process, electroless plating process, electrical resistance measurement and printing of complex patterns. This material is available free of charge via the Internet at http://pubs.acs.org.

■ AUTHOR INFORMATION

Corresponding Author

*E-mail: singler@binghamton.edu. Tel: +01 607-777-4330. Fax: +01607-777-4620;.

Notes

The authors declare no competing financial interest.

■ ACKNOWLEDGMENTS

This research was supported in part by the Analytical and Diagnostics Laboratory (ADL) in the Small Scale Systems

Integration and Packaging Center (S3IP) at SUNY Binghamton. The authors would like to thank Mr. Heng Yang and Dr. M. Stanley Whittingham of the Institute for Materials Research at SUNY Binghamton for use of their x-ray diffraction system and for technical support.

REFERENCES

(1) Angmo, D.; Larsen-Olsen, T. T.; Jørgensen, M.; Søndergaard, R. R.; Krebs, F. C. Roll-to-Roll Inkjet Printing and Photonic Sintering of Electrodes for ITO Free Polymer Solar Cell Modules and Facile Product Integration. *Adv. Energy Mater.* **2013**, *3*, 172−175.

(2) Janoschka, T.; Teichler, A.; Häupler, B.; Jähnert, T.; Hager, M. D.; Schubert, U. S. Reactive Inkjet Printing of Cathodes for Organic Radical Batteries. *Adv. Energy Mater.* **2013**, *3*, 1025−1028.

(3) Dua, V.; Surwade, S. P.; Ammu, S.; Agnihotra, S. R.; Jain, S.; Roberts, K. E.; Park, S.; Ruoff, R. S.; Manohar, S. K. All-Organic Vapor Sensor Using Inkjet-Printed Reduced Graphene Oxide. *Angew. Chem., Int. Ed.* **2010**, *49*, 2154−2157.

(4) Shin, K.-Y.; Hong, J.-Y.; Jang, J. Micropatterning of Graphene Sheets by Inkjet Printing and Its Wideband Dipole-Antenna Application. *Adv. Mater.* **2011**, *23*, 2113−2118.

(5) Schindler, A.; Brill, J.; Fruehauf, N.; Novak, J. P.; Yaniv, Z. Solution-Deposited Carbon Nanotube Layers for Flexible Display Applications. *Phys. E (Amsterdam, Neth.)* **2007**, *37*, 119−123.

(6) Singh, M.; Haverinen, H. M.; Dhagat, P.; Jabbour, G. E. Inkjet Printing-Process and Its Applications. *Adv. Mater.* **2010**, *22*, 673−685.

(7) Krebs, F. C.; Fyenbo, J.; Jørgensen, M. Product Integration of Compact Roll-to-Roll Processed Polymer Solar Cell Modules: Methods and Manufacture Using Flexographic Printing, Slot-Die Coating and Rotary Screen Printing. *J. Mater. Chem.* **2010**, *20*, 8994.

(8) Noh, J.; Yeom, D.; Lim, C.; Cha, H.; Han, J.; Kim, J.; Park, Y.; Subramanian, V.; Cho, G. Scalability of Roll-to-Roll Gravure-Printed Electrodes on Plastic Foils. *IEEE Trans. Electron. Packag. Manuf.* **2010**, *33*, 275−283.

(9) Kamyshny, A.; Magdassi, S. Conductive Nanomaterials for Printed Electronics. *Small* **2014**, *10*, 3515−3535.

(10) Reinhold, I.; Hendriks, C.; Eckardt, R.; Kranenburg, J.; Perelaer, J.; Baumann, R.; Schubert, U. Argon Plasma Sintering of Inkjet Printed Silver Tracks on Polymer Substrates. *J. Mater. Chem.* **2009**, *19*, 3384.

(11) Ma, S.; Bromberg, V.; Liu, L.; Egitto, F. D.; Chiarot, P. R.; Singler, T. J. Low Temperature Plasma Sintering of Silver Nanoparticles. *Appl. Surf. Sci.* **2014**, *293*, 207−215.

(12) Ko, S. H. S. H.; Pan, H.; Grigoropoulos, C. P. C. P.; Luscombe, C. K. C. K.; Fréchet, J. M. J. J. M. J.; Poulikakos, D. All-Inkjet-Printed Flexible Electronics Fabrication on a Polymer Substrate by Low-Temperature High-Resolution Selective Laser Sintering of Metal Nanoparticles. *Nanotechnology* **2007**, *18*, 345202.

(13) Jang, S.; Lee, D. J.; Lee, D.; Oh, J. H. Electrical Sintering Characteristics of Inkjet-Printed Conductive Ag Lines on a Paper Substrate. *Thin Solid Films* **2013**, *546*, 157−161.

(14) Perelaer, J.; Abbel, R.; Wünscher, S.; Jani, R.; van Lammeren, T.; Schubert, U. S. Roll-to-Roll Compatible Sintering of Inkjet Printed Features by Photonic and Microwave Exposure: From Non-Conductive Ink to 40% Bulk Silver Conductivity in Less than 15 Seconds. *Adv. Mater.* **2012**, *24*, 2620−2625.

(15) http://www.metalprices.com.

(16) Deng, D.; Cheng, Y.; Jin, Y.; Qi, T.; Xiao, F. Antioxidative Effect of Lactic Acid-Stabilized Copper Nanoparticles Prepared in Aqueous Solution. *J. Mater. Chem.* **2012**, *22*, 23989.

(17) Grouchko, M.; Kamyshny, A.; Magdassi, S. Formation of Air-Stable Copper−silver Core−shell Nanoparticles for Inkjet Printing. *J. Mater. Chem.* **2009**, *19*, 3057.

(18) Rozenberg, G. G.; Bresler, E.; Speakman, S. P.; Jeynes, C.; Steinke, J. H. G. Patterned Low Temperature Copper-Rich Deposits Using Inkjet Printing. *Appl. Phys. Lett.* **2002**, *81*, 5249.

(19) Kamyshny, A. Metal-Based Inkjet Inks for Printed Electronics. *Open Appl. Phys. J.* **2011**, *4*, 19−36.

(20) Mallory, G. O.; Hajdu, J. B. *Electroless Plating: Fundamentals and Applications*: 1st ed; William Andrew: Norwich, NY, 1991.

(21) Busato, S.; Belloli, A.; Ermanni, P. Inkjet Printing of Palladium Catalyst Patterns on Polyimide Film for Electroless Copper Plating. *Sens. Actuators, B* **2007**, *123*, 840−846.

(22) Chang, Y.; Yang, C.; Zheng, X.-Y.; Wang, D.-Y.; Yang, Z.-G. Fabrication of Copper Patterns on Flexible Substrate by Patterning-Adsorption-Plating Process. *ACS Appl. Mater. Interfaces* **2014**, *6*, 768−772.

(23) Wang, M.-W.; Liu, T.-Y.; Pang, D.-C.; Hung, J.-C.; Tseng, C.-C. Inkjet Printing of a pH Sensitive Palladium Catalyst Patterns of ITO Glass for Electroless Copper. *Surf. Coat. Technol.* **2014**, DOI: 10.1016/j.surfcoat.2014.02.031.

(24) Gysling, H. J. Nanoinks in Inkjet Metallization — Evolution of Simple Additive-Type Metal Patterning. *Curr. Opin. Colloid Interface Sci.* **2014**, *19*, 155−162.

(25) Zhu, P.; Masuda, Y.; Koumoto, K. Seedless Micropatterning of Copper by Electroless Deposition on Self-Assembled Monolayers. *J. Mater. Chem.* **2004**, *14*, 976.

(26) Lee, H.; Dellatore, S. M.; Miller, W. M.; Messersmith, P. B. Mussel-Inspired Surface Chemistry for Multifunctional Coatings. *Science* **2007**, *318*, 426−430.

(27) Yan, J.; Yang, L.; Lin, M.-F.; Ma, J.; Lu, X.; Lee, P. S. Polydopamine Spheres as Active Templates for Convenient Synthesis of Various Nanostructures. *Small* **2013**, *9*, 596−603.

(28) Ma, S.; Liu, L.; Bromberg, V.; Singler, T. J. Fabrication of Highly Electrically Conducting Fine Patterns via Substrate-Independent Inkjet Printing of Mussel-Inspired Organic Nano-Material. *J. Mater. Chem. C* **2014**, *2*, 3885.

(29) Deegan, R. D.; Bakajin, O.; Dupont, T. F.; Huber, G.; Nagel, S. R.; Witten, T. A. Capillary Flow as the Cause of Ring Stains from Dried Liquid Drops. *Nature* **1997**, *389*, 827−829.

(30) Bromberg, V.; Ma, S.; Singler, T. J. High-Resolution Inkjet Printing of Electrically Conducting Lines of Silver Nanoparticles by Edge-Enhanced Twin-Line Deposition. *Appl. Phys. Lett.* **2013**, *102*, 214101.

(31) Liao, Y.-C.; Kao, Z.-K. Direct Writing Patterns for Electroless Plated Copper Thin Film on Plastic Substrates. *ACS Appl. Mater. Interfaces* **2012**, *4*, 5109−5113.